Eco-Toxic Risk Assessment of Nearshore Sediments in Bay of Bengal - Environmental Radioactivity and Ecological Risk as a Proxy

Manikanda Bharath K (Krmanibharath93@gmail.com)
National Institute of Technical Teachers' Training and Research Chennai https://orcid.org/0000-0002-3159-8098

Usha Natesan
National Institute of Technical Teachers' Training and Research Chennai

Chandrasekaran Seethapathy
IGCAR: Indira Gandhi Centre for Atomic Research

Srinivasalu Seshachalam
Anna University Chennai

Research Article

Keywords: Nearshore sediments, environmental radioactivity, toxic elements, potential ecological risk, geospatial tools, pollution assessment.

Posted Date: March 22nd, 2022

DOI: https://doi.org/10.21203/rs.3.rs-1454882/v1

Eco-toxic risk assessment of nearshore sediments in Bay of Bengal - Environmental radioactivity and ecological risk as a proxy

Manikanda Bharath Karuppasamy[1,2]*, Usha Natesan[2]*, Chandrasekaran Seethapathy[3], Srinivasalu Seshachalam[1]

[1] *Institute for Ocean Management, Anna University, Chennai – 600025, Tamil Nadu, India, (https://orcid.org/0000-0002-3159-8098).*

[2] *National Institute of Technical Teachers Training and Research (NITTTR) Chennai – 600113, Tamil Nadu, India.*

[3] *Radiological Safety Division Health Safety and Environmental Group, Indira Gandhi Centre for Atomic Research, Kalpakkam-603102, Tamil Nadu, India.*

*Corresponding authors: krmanibharath93@gmail.com; u_natesan@yahoo.com

Abstract

The present study focuses on the environmental radioactivity and multi-risk assessment of nearshore sediments as a source of marine pollution along the Bay of Bengal. The study examines the distribution of primordial radionuclides concentration using a Na(I)Tl detector-based gamma-ray spectrometer and Potentially Toxic Elements (PTE) through atomic adsorption analysis. Further, the data obtained and characterization radiological risks, ecological threats, and assessing the spatial distribution of toxic elements in nearshore sediments as a proxy for marine contamination. The active concentration of primordial radionuclides such as ^{238}U, ^{232}Th and ^{40}K were found in ranged from ≤ 3 to 68 (11.4), ≤ 9.5 to 142.7 (41.2) and 85.2 to 603.4 (362) Bq kg^{-1}. Results show that the concentration of the average radionuclides is less than suggested by UNSCEAR ranges. The concentration of potentially toxic elements (Fe, Cr, Ni, Pb and Zn) was higher in deeper water depth. This study exposes that the primary control of such elements is mud distribution. A decreasing order has been seen as follows by the ecological risk index of individual elements: Cu > Pb > Ni > Cr > Zn. The significant Pb, Cu and Zn concentration was polluted at most stations, possibly contributing the regional and terrestrial sources such as industrial activity, urban drainage, manufacturing, and farming. This research suggests that anthropogenic behaviours in nearby land are the source of the deposition of metals and radionuclides in coastal and marine sediments.

Keywords: Nearshore sediments, environmental radioactivity, toxic elements, potential ecological risk, geospatial tools, pollution assessment.

1. Introduction

Sediments in the benthic zone play an essential part in coastal and marine ecosystems. The assessment of ecological and radiological risks is determined by the indicators of marine surface sediments. Heavy metal and radionuclide concentrations in coastal sediments originated from both the geogenic (physical and chemical rock weathering) and anthropogenic process (Ghias et al. 2021). Primordial radionuclides and potentially toxic elements in coastal sediments are capable of providing some valuable information regarding the source, components of transport and the nature of marine environments, where it may be predicted as a serious environmental concern (Khan et al. 2021). Geochemical cycling of different elements in the aquatic environments has significant ecological effects on food-web driven pollution that will enter the whole biota, which has been significantly altered by the possibility in coastal regions, urban emissions, and industrial activities worldwide (Magesh et al. 2011, Wang et al. 2020). Environmental pollution measurement in the marine environment is determined by the amount of seawater residual particulate matter, rate of particular primordial radionuclides in the sediments and possibly radioactive materials (Inigo Valan et al. 2020; Thangam et al. 2020). This investigation shall provide valuable information for controlling natural radioactivity and toxic element's pollution in the coastal environments (Yii et al. 2009; Adam, and Eltayeb (2012); Zhang et al. 2016). Some of the expected anthropogenic behaviour contributing to the release of pollutants into the coastal and marine environment like potentially toxic elements and primordial radionuclides are effluent from fertilizer, oil refineries, municipal sewages and urban wastewater treatment plants, spills in shipping and port activities, extensive agricultural activities, leakage of oil from off-shore, riverbeds discharge contains the natural and anthropogenic element species (Sylaios et al. 2012; Stamatis et al. 2019). Several kinds of research have also been established that the sediments are particularly susceptible to trace elements concentration in coastal zones and thus initiates the awareness of marine contaminants by assessing their trace metal accumulation in the sediments (Jayaprakash et al. 2008; Huang et al. 2015). Among the pollutants in marine sediments, Potentially Toxic Elements (PTE) and primordial radionuclides are the major threat to the environmental system due to their toxicity and biological accumulation (Maanan et al. 2015; Sérgio et al. 2021). Methods were established to identify the main reasons for improved risk assessments. The usage of surface sediment indices in marine environments is the primary tool used to determine the environmental condition (Zhou et al. 2020)**.** Accumulation and dissemination of natural

radioactive elements often useful for the detection of natural radioactivity of environmental contamination (UNSCEAR, 2000; Taieb Errahmani et al. 2020). The progeny radioactivity of the typical decay sequence cannot be in considerable equilibrium with their parents in the marine ecosystem (IAEA, 2003). The weathering and deposition of minerals in surface rocks are the primary causes of environmental radioactivity (Koide et al. 1973).

In recent years, research reveals that increased background radiation in the environment is the primary importance for risk assessment related to long-term low average body exposures to the public. The study of primordial radionuclides and the distribution of toxic substances allows an evaluate the radiological and ecological impact of various radioactive material and harmful elemental pollutants in the seafloor environment. Environmental radioactivity is related to the exposure of gamma-rays to the organism and even from the inhalation of radioactive substances such as radon and its daughters into the respiratory system. In the last few years, the Coromandel coast of India has seen dramatic changes and developments of major industrial activities, urbanization, transportation, shipping, tourism and aquaculture. Radiological studies conducted in beach and marine sediments at several locations on the south-eastern coast of India. The report recommended the presence of monazite and zircon concentrations traverse the shore, generating natural background radiation exposure to people living on and around the Coromandel coast of India. This study examines the active concentrations of radioactive elements such as ^{238}U, ^{232}Th and ^{40}K in marine sediments and it will help to identify the radiological threats in coastal environments. The ecological risk assessed by the radioactive elements and radiological risk parameters such as the Radium Equivalent Activity (Ra_{eq}), Absorbed Dose Level (D_R), Annual Effective Dose Ratio (AEDR) and External Risk Index (H_{ex}) may be determined from the data obtained. The data collected from the sample can relate to the level of natural radioactivity and the level of toxic contaminants in the sediments

This study aimed to focus on assessing the concentration of primordial radionuclides and trace elements that can occur from the effects of buried or movable sediments along the Bay of Bengal. Multi-risk assessments were carried out, such as ecological threats, radiological risks and assessing the spatial distribution of toxic elements in nearshore sediments as a proxy for marine contamination. Therefore, it was necessary to monitor the levels of gamma radiation and ecological risk along the shore and to assess the potential radiation dose rates ingested by marine organisms.

2. Study area details

The Figure 1. represents the area of interest and sampling of marine sediments. The study area covers 180 km which is situated on India's coromandel coast. Two major ports– Chennai and Ennore Port are located in the study zone. The wind speed is about an average of 14.82 km/h during the year. The parameters to monitor sediment flow on the Southeast coast are water current, wave action and the geomorphological feature. A smaller port is used by fishing vessels and trawlers at Royapuram. A large number of sewages from the Chennai Area, due to rapid industrialization and urbanization, causing significant river pollution. Marina beach which locates between the port of Chennai and the estuary of Adyar river, Kovalam Beach, a tourist area that invites tourists from across the world which is located 40km away from south of marina beach and near to (3.3 km) the backwaters of Muttukadu which is a tourist boat destination. Apart from trading and transport, Chennai majorly considers the electronic, manufacturing, automotive, medical treatment sectors. The backwaters of Muttukadu often get large quantities of industrial waste, eventually released into marine wetlands. Kalpakkam which is situated 65 km away from south of Chennai, has a major nuclear power plant complex consists of Madras Atomic Power Station (MAPS), a Fast-Breeder Test Reactor (FBTR) and the Indira Gandhi Center for Atomic Research Centre (IGCAR), a Central Waste Management Facilities (CWMF) and a Development and reprocessing Laboratory (DRL). In the coastal region, the three seasonal behaviors in a year, like October-January during North-East monsoon, South-West monsoon in June–September, and Non-monsoon in February-May exhibits numerous morpho-dynamic activities which were observed by the locals. Thus, these were the reason for selecting a character-based sampling location from the urban and domestic effluent discharge point.

3. Materials & Methods

3.1. Sampling and sample preparation

The sediment samples were carefully collected in the continental shelf area along the coast of Tamil Nadu from seven transects by a grab sampler of Van Veen grab (dimensions 40 × 40 cm), from Pulicat lake to Kalpakkam along the coromandel coast in India, during pre-monsoon season in the Bay of Bengal. A collection of 26 sediment samples obtained from CRV Sagar Purvi, IMO cruise number 9123829 on 26 cross transects around the study area shelf region took place on a cruise in November 2018 (Fig.1). General Bathymetric Contour maps of the Oceans (GEBCO 2019) data were applied to low water areas in Bengal by contorting

them inflexible mesh bathymetry to each dimension in the depth of waters and improved bathymetry measurement systems. The bathymetry and topography collected during the field survey were applied to nearshore coastal areas, whereas the single beam echosounder was applied to the deep-water regions it's given in the supplementary information of Fig. S1.

The horizontal datum was referenced to World Geodetic System 1984 UTM Zone 44N and the vertical datum was referenced to Mean Sea Level (MSL). The bathymetry and topography collected during the field survey were applied. Sediment Samples from the seabed were collected at varying depths of 20 m to 430 m water depth ranging near shore to off-shore from 26 stations (Fig. 1). Each sampling site situated with an average of 5 NM. (nautical mile) and samples weighing about 1 kg was preserved in a polythene bag. Individually collected marine sediments were initially dried in open-air at room temperature in the laboratory and then oven-dried at 100°-110°C aimed at 24 hours to obtain constant weight. The calcium carbonate ($CaCO_3$), organic matter (OM) and organic content (OC) for coastal sediments were measured in Gaudette et al., 1974, Muller and Suess 1979 and Loring and Rantala methods (1992). The size of the sediments was analysed using particle size analyser (Laser Malvern Master sizer 2000). The particle size analytical capability of the instrument ranges between 0.1-2000µm respectively, with a 0.5 resolution. From the Oven-dried samples, one part of the sediments was segregated for carrying out Trace element analysis and the other for the determination of radionuclides using the standard procedures. The 0.5g of homogeneous sediment sample powdered and preserved in Tephlon bombs and then subjected to acid digestion in the proportion of 3:2:1 (HNO_3: HCl: H.F) respectively by Loring and Rantala (1992). After this digestion; the trace elements were analysed through an atomic absorption spectrometer (Perkin Elmer AA800) at Anna University, Chennai. Minimum detection limits (LOD) for Fe, Zn, Cr, Cu, Ni and Co are 0.01 µg/L for Mn 0.02 µg/L and Pb 00.5 µg/L. Gamma spectrometry was used to assess radioactivity of ^{232}U, ^{232}Th, and ^{40}K for sediments, utilizing a NaI (Tl) detector through a small baseline at 3-inch/3-inch NaI detector (Tl) (AQCS 1995; IAEA 2003). The adequate lead shielding coupled to 8K multichannel analyzer in the laboratory Radiation Safety Division, Indira Gandhi Centre for Atomic Research, Kalpakkam was employed were investigated for present work. For reference, the calibration is made in the device using Uranium Ore Sample (RGU-1), Thorium Ore Sample (RGTh-1) and a Potassium Sample (RGK-1) obtained from IAEA (International Atomic Energy Agency) (Ramasamy et al., 2009, Senthilkumar et al., 2010 and Belyaeva et al., 2021). Based on the background radiation spectrum of three radionuclides itself were calculated Below detectable limit (BDL).

The details of these reference materials can be referred to in IAEA and AQCS (1995). For a total of 20,000 seconds of measurement in the framework for each marine sediment sample, the detection limit at NaI (Tl) detector for ^{238}U, ^{232}Th and ^{40}K was in 2.21, 2.11 and 8.50 Bq/kg (Ravisankar et al. 2014; Tholkappian et al. 2017). The gamma-ray spectroscopy photo-peak correspondingly to 1460 keV for ^{40}K, 1764 keV for ^{214}Bi and 2614 keV for ^{208}Tl the appearance at the activity was considered of ^{40}K, ^{238}U (^{226}Ra) and ^{232}Th in the sediment samples (Beretka and Matthew (1985); Tholkappian et al. 2018; Thangam et al. 2020). The results were statistically analysed, and the geospatial distribution of radiological hazards and ecological risk data set has been done using the spatial tools analysis module in Arc GIS 10.7.1, GeoDa and Microsoft excel 2016.

4. Results and Discussion

4.1. Primordial radionuclide activity concentration in the nearshore sediments

Spatial distribution of environmental radioactivity (^{238}U,^{232}Th and ^{40}K) levels from different locations in the study region in marine sediment samples, are shown in Fig. 2. The activity of Uranium, Thorium and Potassium shows an average value range from $\leq 3 - 68$ (11.4), $\leq 9.5 - 142.7$ (41.2) and 85.2 – 603.4 (362) Bq kg^{-1} in the offshore sediments are shown in Fig. 2. The primordial radionuclide measurements ranged significantly, depending on their physicochemical and geochemical condition of the activities in the coastal and marine environment (Maanan et al. 2015). Concentrations of activity were in the range of $^{40}K > ^{232}Th > ^{238}U$ for all samples. It was also observed that Potassium (^{40}K) activity concentration was higher in the samples than that of radium and thorium. Results show that the concentration of average radionuclides is less than suggested by (UNSCEAR, 2000; IAEA, (2003)) and is smaller than its maximum (world average of ^{232}Th is 45 and ^{238}U is averages of 32 is Indian an average between 29 and 64 Bq/kg), which are opposed to ^{40}K well within the worldwide recommended limit and also Indian limit of 420 Bq/kg. The Potassium (^{40}K) activity level was probably higher in the soil because of micronutrients. Mobilization and subsequent migration might be the reason for the increased value in ^{238}U (Yii et al. 2009; Thangam et al. 2020). The radionuclides depositional environments of the study area showing continental to marine zones it given in the Fig. 2. The maximum radiological activities reflect in the nearshore environments such as inner neritic zone up to 35m water depth in shallow marine region only.

The radium equivalent activity (Ra_{eq}) is a standard quantity index to be implemented for common ^{238}U, ^{232}Th and ^{40}K activity, taking into consideration their related radiation risks and

the overall concentration in Ra_{eq} essential about 370 Bq/kg. According to Beretka and Mathew, (1985), this index determined:

$$\mathbf{Ra_{eq} = A_U + 1.43A_{Th} + 0.077A_K \leq 370\ Bq/kg}$$

Where ^{238}U, ^{232}Th and ^{40}K in Bq/kg are specific behaviours of Active concentration of A_U, A_{Th} and A_K. Outdoor naturally absorbed gamma dose rates were measured at radioactivity of ^{238}U, ^{232}Th and ^{40}K dependent on terrestrial radiation at a height above ground level of 1 m. The allowed value of Ra_{eq} activities was 370 (Bq/kg), and efficient dose in 1 mSv/yr for the environment inhabitants in the ecosystem (IAEA, 2003; Tholkappian et al. 2018). In such marine sediment samples, Radium Equivalent Activity (Ra_{eq}) levels range from 31.51-243.21 Bq/kg on average and around 95.6 Bq/kg. The mean value of radium equivalent activity was shows in much lesser than recommended value (370 Bq/kg) (UNSCEAR, 2000). The results indicated that the radium equivalent is increasing as we move towards the shore, based on water depth it's shown in Fig. 3. Sediments from Pulicat shore registered the highest Ra_{eq} activity as compared to other sediments, and also the variation of an average value of Radium equivalent was plotted with distance from onshore in Fig. 3. So, these may be the pollutants derived from inland to the nearshore region due to the activity of urban effluents.

4.2. Radiological threat evaluation

4.2.1. Gamma dose rate (D_R)

The gamma dose rate for randomly distributed energy from ionizing surface radiation in the soil is one of the essential techniques for risk analysis (Gbadamosi et al. 2018). The UNSCEAR 2000 introduced different models in various papers for the transfer of radionuclides from the surface level above 1m of activity levels ^{238}U (^{226}Ra), ^{232}Th and ^{40}K (Bq kg^{-1}) to gamma dose rate in nano Gray h^{-1} from total radionuclide exposure of 1 meter from surface radiation (Huang et al. 2015; Ghias et al. 2021). This aspect adapts to the life cycle in the study region and provides effective dosage level outdoors (Inigo Valan et al. 2020; Thangam et al. 2020). The UNSCEAR conversion factor was introduced, and the rate of the gamma dose rate was calculated using the below equation (UNSCEAR, 2000).

$$\mathbf{D_{soil} = 0.427A_U + 0.662A_{Th} + 0.0432A_K}$$

With a mean of 45.3 nGy h^{-1}, the gamma-dose ranged between 14.59 and 109.19 nGy h^{-1}. Figure 3. shows the gamma dose spatial variation in sampling sites.

4.2.2. Annual Effective Dose Equivalent (AEDE)

The average annual effective dosage was calculated using 0.7 Sv Gy conversion to an actual equivalent dose and 0.2 for outside occupancy (Zhou et al. 2020). the dose rate is estimated to be absorbed. The percentage transfer of a dosage consumed in the soil to an appropriate dose and the level of outdoor occupation will be assessed. Efficient dose equivalent (mSv y^{-1}) was determined by (UNSCEAR, 2000; Taieb et al. 2020):

$$\mathbf{AEDE_{out}\ (mSv/y) = D\ (nGy/h) \times 24\ hours \times 365\ days \times 0.2 \times 0.7\ (Sv/Gy) \times 10^{-6}}$$

The AEDE was calculated to be 0.02-0.13 mSv y^{-1}, with a mean of 0.056 mSv/y, even smaller than the global average at 84 $nGyh^{-1}$ by UNSCEAR, 2000. Fig. 3 shows the annual effective dose equivalent (AEDE) spatial variability at various locations around the entire sample region.

4.2.3. Activity Utilization Index (AUI)

A sediment Activity Utilization Index (AUI) has been developed to facilitate the calculation by using the following formula of air exposure rates from the various mixtures of the three radionuclides (Zhou et al. 2020; Khan et al. 2021):

$$\mathbf{AUI} = \left(\frac{\mathbf{A_U}}{\mathbf{50\,\frac{Bq}{kg}}}\right)\mathbf{f_U} + \left(\frac{\mathbf{A_{Th}}}{\mathbf{50\,\frac{Bq}{kg}}}\right)\mathbf{f_{Th}} + \left(\frac{\mathbf{A_K}}{\mathbf{500\,\frac{Bq}{kg}}}\right)\mathbf{f_K}$$

The fractional contributions from overall air dose levels are attributed from the gamma radioactivity and the total activity of these radionuclides are A_U, A_{Th} and A_K in Bq/kg of uranium (^{238}U), thorium (^{232}Th) and Potassium (^{40}K), and f_U (0.462), f_{Th} (0.604), and f_K (0.041) respectively. According to (Belyaeva et al., 202), typical activities were defined as 50 and 500 Bq kg^{-1}, for each mass of unit ^{238}U,^{232}Th and ^{40}K and A_U, A_{Th} and $A_{K.}$ sediments. Fig. 3 shows the spatial variation of AUI in different locations in the sampling sites. The AUI ranged from 0.17-1.79 mSv/y, mean of 0.63 mSv/y was calculated in this study. The mean value of AUI is 0.63 which is also less than the recommended value (<2) (Ramasamy et al. 2009; Senthilkumar et al. 2010).

4.2.4. External hazard index (H_{ex})

The External Risk Index (Hex) is another radiation risk indicator identified according to Beretka and Mathew 1985 for the estimation of the indoor radioactivity risk in construction material for dwellings as a consequence of direct exposure to natural radionuclide radioactive (Ravisankar et al. 2014; Tholkappian et al. 2017). The index value of the radiation risk should

be less than unity, i.e. the exposure to radiation by building materials should be reduced at 1.5 mSv/y depending on the following criteria:

$$H_{ex} = \frac{A_{Th}}{259Bq/kg} + \frac{A_U}{370Bq/kg}\frac{A_K}{4810Bq/kg} \leq 1$$

Where the activity of ^{238}U, ^{232}Th and ^{40}K are respectively A_U, A_{Th} and A_K in Bq/kg. The H_{ex} amount must be less than unity to continue the Negligible amount of radiation risk. Using the above equation H_{ex}, as shown in Figure 3, we can conclude from the figure that H_{ex} contained in this analysis was between 0.086 and 0.66, with an average of 0.265. In the present sample region, the values for H_{ex} with a mean of 0.26 are lower than the acceptable limit (<1) and less than 0.3 in soil (Tholkappian et al. 2018; Sérgio et al. 2021). This ensures the sediment samples are healthy and not heavy in radiation levels. A similar study was reported in the coastal sediments at Chennai Coast, Tamil Nadu, India by (Tholkappian et al. 2017; Inigo Valan et al. 2020), whose H_{ex} concentration indicating that marine sediment external threat index levels have not reached the permissible limit.

4.2.5. Internal hazard index (H_{in})

Another hazard index is defined, the Internal Hazard Index (H_{in}), Radon is toxic to the respiratory organs, along with its short-lived by-products (Koide et al. 1973; Adam et al. 2012). Radon and the daughter products have their environmental exposures and quantified, suggested by (Gbadamosi et al. 2018; Belyaeva et al. 2021). The average permissible limit of ^{238}U (^{226}Ra) to half of the value was acceptable for the external exposure only, and index is established:

$$H_{in} = \frac{A_{Ra}}{185Bq/kg} + \frac{A_{Th}}{259Bq/kg} + \frac{A_K}{4810Bq/kg}$$

To decrease internal activity and its radioactive progeny, the H_{in} had been included. In the present study region, the values for H_{in} with a mean of 0.29 are lower than the acceptable limit (<1) and less than 0.3 in soil, it shows in Fig. 3. In the sediment samples, all radiological parameters assessed are lower than acceptable, except for the certain areas Kalanji (S1), Muttukadu (S22), and Kalpakkam (S24) near to the activity rate of the primordial radionuclides. It could be the presence of heavy minerals and rich black Sand in the areas.

4.3. Sedimentological characteristics of the study area

The Sedimentological and granulometric characteristics in the study region showed (Fig. 4). The seawater that passes through the channel remains in the mouth of the flocculated sediments and transfers the delicate flocculation to the water column (Wang et al. 2011). The

small particles from the fluvial mouth are often played a direct impact on the tidal currents. The movement of long-shore drift and debris had led to the sediment transport of Sand and silt particles on the off-shores (Muller and Suess (1979)). The word organic matter is used to denote the part of the sediment formed by organic activities comprising of carbon another carbonate (Bonnail et al. 2016). It can be named "marine humus" since it's a little similar to the humus fraction in soils (Li et al. 2018). The spatial diagram for the distribution of sand-silt-clay ration, calcium carbonate, organic carbon and organic matter shows explicitly that they are produced from ocean drift to the off-shore by way of long-shore drifting sediments (Fig. 4). The granulometric characteristics of collected sediment's as given supplementary information of Fig. S2. The distribution of pollutants in industrial surface sediments is not compatible with the regulation on hydro-dynamics of natural environments such as beaches and rivers (Abrahim and Parker, (2008)). The overall measurements of heavy metals at the south zone were high in comparison towards the north of the sampling region. These rivers carry massive quantities of sediments through an anthropogenic and geogenic process which are dumped in the coastal area (Gan et al. 2000). The heavy metal concentration and statistical summary show on the Box and Whisker Plot in Fig. 5. The concentration of trace elements (Fe, Cr, Ni, Pb and Zn) were higher in deep water, some portions of the sediments were muddy due to high organic matter. The concentration of Co and Cu increased in shallow depth portion containing more-sandy. The strong association among metals such as Cu, Ni, Pb and Zn and mud portion indicate they're becoming mainly mud (silt+ clay) (Tian et al., 2017). This study exposes that the primary control of such elements is mud distribution. The significant Pb, Cu and Zn concentration was polluted at most stations, possibly contributing to the regional and terrestrial sources (such as industrial, urban drainage, manufacturing, and farming).

4.4. Heavy metal risk evaluation

4.4.1. Sediment pollution index (SPI)

The SPI ratio proposed by (Hakanson, 1980; Magesh et al., 2011; Tian et al., 2017) to evaluate the nature of the sediment and the metal toxicity of trace elements become exposed. The determine the SPI by the following equations:

$$\mathbf{SPI} = \sum (\mathbf{Cf_m} \times \mathbf{W_m}) / \sum \mathbf{W_m}$$

For Cfm the ratio of the concentration of determined metals (Cn) to metal background concentration with Wm is the weight of toxicity. The Hakanson, 1980 proposed the

concentration of toxic weight one at Cr and Zn, 5 for Pb, Cu and Ni, respectively. Based on the value the sediments were categorised: 0–2 = natural sediment, 2–5 = low polluted sediment, 5–10 = moderately polluted sediment, 10–20 = highly polluted sediment, and > 20 = dangerous sediment. Fig. S3 shows the spatial variability of the SPI in the sampling site concentration of metals in marine sediments as given in the supplementary information. The sediment pollution index ranged from 10 to 52, with an average of 25. Moreover, the SPI report presented that the sediments were very contaminated, but not in the dangerous sediment category.

4.4.2. Contamination factor (CF) & Degree of Contamination (CD)

The Contamination factor (CF) and the degree of contamination (CD) were used to assess the anthropogenic effect on sediment chemistry and to calculate the concentration of metals in the sediment sample towards uncontaminated baseline values metal (Taylor and Mclennan (1995); Stamatis et al., 2019; Wang et al. 2020). As reported in Hakanson, (1980), CF is the ratio for specific metals in soil and its background. Although the C.F. value for the individual elements is determined, the CD contains full information on the sample sites that contaminates sediment. The expressions CF and CD are:

$$\mathbf{CF} = \frac{\mathbf{C_m}}{\mathbf{C_b}}$$

The contaminant of the CF < 1 (low contamination), the CF < 3 (moderate pollution), the CF < 6 (substantial contamination) and the CF > 6 (very high pollution) were listed by (Hakanson, 1980). Fig. 5. shows spatial variation of the contamination factor at sediments of the region analysed for the concentration of the element. In addition to Co > Cu > Cr > Ni > Ni > Pb > Zn > Mn provided Fig. 5; the contaminant factor values were reported. The sediment samples in this field were categorized based on the C.F. as medium contaminated that ranges between 0.1 and 14 with a mean value of 3. Hakanson, (1980) proposed the investigating method of Degree of Contamination (CD) towards permit pollution control easier. The categorization of pollution is proposed by (Hakanson, (1980); Pejman et al. 1995) when CD < 6 (low level of pollution), 6 < CD 12, (moderate levels of contamination), 12 < CD < 24, (considerable level of contamination). The description of the CF for each element concerned was described as below:

$$\mathbf{CD} = \sum_{\mathbf{i=1}}^{\mathbf{n}} (\mathbf{CF})$$

Fig. 5 showed the Spatial variation of Contamination Degree (CD) for metals in the sampling sites. The degree of contamination ranged from level 9 to 52 with an average of 27, so CD classification indicated that the sediments from this study area lie in the High contamination category.

4.4.3. Pollution Load Index (PLI)

The PLI was to assess the total contamination of sediments by the pollutants at the studied sites. PLI provided an assessment of metal contamination and the actions required. The following method is necessary to measure the PLI (Tomlinson et al. 1980; Taylor and Mclennan 1995; Tian et al. 2017).

$$\mathbf{PLI} = (\mathbf{CF1} \times \mathbf{CF2} \times \ldots\ldots\ldots\ldots\ldots \times \mathbf{CFn})^{\frac{1}{n}}$$

Where n was the cumulative number of metals (CF) tested. The PLI values nearby to 0 or 1 to specify the current pollutants 'degree of perfection or baseline, but PLI values > 1 showed progressive deterioration in the study region (Jayaprakash et al. 2008; Ramasamy et al. 2009, Tholkappian et al. 2017; Inigo Valan et al. 2020). Spatial variability of the Pollution Load Index (PLI) for the concentration of metals at sampling sites in marine sediments was shown in Fig. 5. The PLI value ranged from 1 to 2, with an average of 1.

4.4.4. The Geo-accumulation index (Igeo)

The Igeo Index reflects the impact of human factors on the environmental and geochemical background (Taylor and Mclennan, (1995). The geo-accumulation factor (Igeo) determined by the below calculation, according to (Hakanson 1980; Magesh et al. 2011).

$$\mathbf{I_{geo}} = \mathbf{log_2}\left[\frac{\mathbf{C_n}}{(\mathbf{1.5} \times \mathbf{C_{bn}})}\right]$$

Where Cn and Bn are the measured element concentration and the background of the element and ‘n’ indicates the Earth’s crust mean (Hakanson, 1980), the factor of 1.5 is the lithogenic impact matrix correction component (Taylor and Mclennan, (1995). In the current research, however, Fe is used to normalize the heavy metals (Pejman et al. 2015; Li et al. 2018). Igeo is graded as "uncontaminated" (Igeo = 0), uncontaminated and lightly polluted (0 < Igeo = 1), slightly to moderately polluted (1 < Igeo = 2), severe to severely polluted (2 < Igeo > 3), strongly polluted (3 < Igeo = 4), strong to seriously polluted (4 < Igeo = 5), or strongly polluted (Igeo > 5) and this Statistical summary was given in **Table 1.** The Igeo based sediment classes were classified and the present environmental situation and metals in the sampling sites were

observed and lie in the fourth category of moderately polluted towards strongly polluted. The presence of Sand in the coastal area was related to the contribution of territorial matter that involves waste from the untreated domestic waste and industrial waste. In the sampling sites, the high energy state and maximum organic material concentration were reported. The mean concentration value of heavy metals in the research area was less than the average background amounts except for Co and Pb (Tomlinson et al., 1980). In this scenario, the contaminating factor (CF) & geo-accumulation index (Igeo) in both Co and Ni have shown that Co and Ni have a high contaminating field of research area due to industrial effluent, boats and ships, fertilizers by farming activities. The Pb, Cu and Zn exposure element and the geo-accumulation index has demonstrated mild sediment pollution from anthropogenic factors, such as oil spills, ships, anti-corrosive marine paints for boats and agricultural fertilizer have been infected.

4.5. Evaluating the pollution status & Potential ecological risk parameter

The researchers have developed this ecological risk model to study the class of sediment pollution based on the toxicity for metals and environmental reaction (Stamatis et al. 2019). potential ecological risk index describes the degree of exposure to toxicity in the specified material for a range of biological populations and details the potential environmental threats posed by harmful metals in the equations (Zhou et al. 2020). The critical role is to classify the type of contaminants and to assign pollution studies (Gan et al. 2000). Soil toxicity was measured in the current study based on the total metal content of selected toxic metals.

$$\mathbf{PRF_i} = \mathbf{TR_i} \times \frac{\mathbf{C_{mi}}}{\mathbf{C_{bi}}}$$

$$\mathbf{PERI} = \sum_{\mathbf{i=1}}^{\mathbf{5}} (\mathbf{PRF_i})$$

Where PERI is classified as a "summation of any risk value of metals in the sediment/soil ". At the same time, TR_i was called a toxic /lethal response factor or toxic response factor. The main risk factor of the pollutant was that of potential risk factor of heavy metals (PRF_i); TRi, the toxic susceptibility of metals; C_{mi}, the metal i content at the sediment; and C_{bi}, the local metal i background value in the sediments. The PERI and PRF_i values were defined by using the following thresholds (Hakanson, (1980); Taylor and Mclennan (1995)). The future hazard from toxic metals emissions is determined with the dangerous analysis of specific metals and environmental exposure against contaminants. TR_i values were estimated at Cu = Pb = 5; Zn = 1; Cr = Ni = 2 (Hakanson, (1980)). The Zhou et al. 2020 reports that the parameters proposed

to Eri are Eri < 40 (low risk), Eri < 80 (moderate risks to ecological conditions), Eri < 160, Eri < 320 (high risks to ecology) and Eri > 320 (very severe ecological risk), respectively, Eri < 40. The words proposed are Eri < 40. The PRF_i and PERI was expressed using the above equations. According to Håkanson, the PERI was defined as having the following five categories: The PERI values were close to PERI < 95 (low environmental risk), 95 < PERI < 190 (moderate environmental risk), 190 < PERI < 380 (significant environmental risk) and PERI > 380 (high ecological risk). In addition to researching the biological processes, PERI methodology covers many fields of work such as toxicology, environmental science, and the identification of environmental risks from toxic metals ((Hakanson, (1980)). The Figure 6 Shows spatial PERI variability for the concentration of elements in sampling sites. The results show specifically PERI which were estimated to be increasing towards off-shore for the anthropogenic sources in the study region shown in Fig. 6. Hence, PERI classification indicated that the sediments that belonged to this study area were perfection and the baseline levels of pollutants provided in Fig. 6. There was a rising sequence of PERI values of individual metals: Cu > Pb > Ni > Cr > Zn. These findings have shown that Cu and Pb posed an increased ecological risk for the study area. When compared with river and flood environment, the organic matter was more in the coastal and marine sediments.

5. Conclusion

In this research the spatial variation of radiological hazards and ecological risk of near shore sediment is taken as a proxy for marine contamination along the Bay of Bengal has evaluated. The specific radioactivity and distribution of primordial radionuclides concentration of ^{238}U, ^{232}Th and ^{40}K was following as ≤ 3 – 68 (an average is 11.4), ≤ 9.5 – 142.7 (41.2) and 85.2 – 603.4 (362) Bq/kg respectively. The occurrence frequency and the average effective dose rate of primordial radionuclides ranged in order $^{40}K > ^{232}Th > ^{238}U$. The results clearly show that the Radium equivalent was estimated to be increasing towards the shore in the study region. Also, recent developments in major industries, the marine sector and port operations have been attributed. The observation of organic matter concentration played an essential part in the movement of nutrients in the environment and water retention at deposits of the study region. The assessment of heavy-metal in sediments at the south-eastern part of Bengal Bay has indicated a high concentration of clay, organic and the deposition of Co, Pb, Cr, Cu, Ni, Zn, Mn, and Fe. A decreasing order has been seen as follows by the ecological risk index of individual elements: Cu > Pb > Ni > Cr > Zn. These studies have demonstrated the enhanced potential ecological threats raised by the marine environment in the sample region by Co, Cu

and Pb. For this study, a measure of radionuclides, the ecological threat of metals and the contrast of reference can be used to help in the future. Ecotoxicity and data collected from this analysis can be useful for the visualization of environmental radioactivity. It can be utilized in future as reference data for the finding of suspected radioactive contaminants.

Acknowledgement:

The authors would like to express deep gratitude for acknowledging **Dr B**. **Venkatraman**, Head, DAE-IGCAR, Radiation Safety Division, Indira Gandhi Centre for Atomic Research, Kalpakkam. DAE-IGCAR for providing funding (Grant Agreement no. IGC/Accts-B&C/IOMAU/RSD-18/2018). We are thankful to the captain, crew, and scientific members of **ORV Sagar Manjusha** sampling; we thank the Ministry of Earth Sciences, Government of India for funds given to the Vessel Management Group, **NIOT Chennai** for providing ship. The technical help received from **Dr. B.V. Mudgal, Director and Dr Kannan Vaidyanathan**, Research associate, IOM, Anna University, and All Technical staffs of Radiological Safety Division Health, Safety and Environmental Group, IGCAR, Kalpakkam, gratefully acknowledged.

References

Abrahim GM, Parker RJ (2008) Assessment of heavy metal enrichment factors and the degree of contamination in marine sediments from Tamaki Estuary, Auckland, New Zealand. Environ Monit Assess.136(1-3):227-38. doi: 10.1007/s10661-007-9678-2.

Adam AM, Eltayeb MA (2012) Multivariate statistical analysis of radioactive variables in two phosphate ores from Sudan. J. Environ. Radioact. 107:23-43. doi: 10.1016/j.jenvrad.2011.11.021.

AQCS (1995) "Intercomparison runs reference materials", Analytical Quality Control Services. IAEA, Vienna.

Belyaeva O, Movsisyan N, Pyuskyulyan K, Sahakyan L, Tepanosyan G, Saghatelyan A (2021) Yerevan soil radioactivity: Radiological and geochemical assessment. Chemosphere. 265:129173. doi: 10.1016/j.chemosphere.2020.129173.

Beretka J, Matthew PJ (1985) Natural radioactivity of Australian building materials, industrial wastes and by-products. Health Phys. 48(1):87-95. doi: 10.1097/00004032-198501000-00007.

Bonnail E, Sarmiento AM, DelValls TA, Nieto JM, Riba I (2016) Assessment of metal contamination, bioavailability, toxicity and bioaccumulation in extreme metallic environments (Iberian Pyrite Belt) using Corbicula fluminea. Sci Total Environ. 544:1031-44. doi: 10.1016/j.scitotenv.2015.11.131.

Gan J, Jia X, Lin Q, Li C, Wang Z, Zhou G, Wang X, Cai W, Lu X (2000) A primary study on ecological risk caused by the heavy metals in coastal sediments. J. Fish. China. 24(6), pp.533-538.

Gaudette HE, Flight WR, Toner L, Folger DW (1974) An inexpensive titration method for the determination of organic carbon in recent sediments. J. Sediment. Res. 44(1), pp.249-253.

Gbadamosi MR, Afolabi TA, Ogunneye AL, Ogunbanjo OO, Omotola EO, Kadiri TM, Akinsipo OB, Jegede DO (2018) Distribution of radionuclides and heavy metals in the bituminous sand deposit in Ogun State, Nigeria–a multi-dimensional pollution, health and radiological risk assessment. J Geochem Explor. 190, pp.187-199.

Ghias S, Satti KH, Khan M, Dilband M, Naseem A, Jabbar A, Kali S, Ur-Rehman T, Nawab J, Aqeel M, Khan MA, Zafar MI (2021) Health risk assessment of radioactive footprints of the urban soils in the residents of Dera Ghazi Khan, Pakistan. Chemosphere. 267:129171. doi: 10.1016/j.chemosphere.2020.129171.

Hakanson L (1980) An ecological risk index for aquatic pollution control. A sedimentological approach. Water Res. 14(8), 975-1001.

Huang Y, Lu X, Ding X, Feng T (2015) Natural radioactivity level in beach sand along the coast of Xiamen Island, China. Mar. Pollut. Bull. 91(1):357-61. doi: 10.1016/j.marpolbul.2014.11.046.

Inigo Valan I, Mathiyarasu R, Lakshmi Narasimhan C, Sridhar SGD, Narayanan V, Stephen A (2020) Mineralogical influence over the presence of primordial radionuclide along the industrial corridor of northern coastal region of Chennai. J. Radioanal. Nucl. Chem. 323(1), 117-133. https://doi.org/10.1007/s10967-019-06956-1.

International Atomic Energy Agency (IAEA) (2003) Guidelines for radioelement mapping using gamma ray spectrometry data (IAEA-TECDOC--1363). International Atomic Energy Agency (IAEA) Vienna (Austria). IAEA-TECDOC-1363. Ref:34083107 (Vol.34). ISSN 1011-4289. http://www-pub.iaea.org/MTCD/publications/publications.asp.

Jayaprakash M, Jonathan MP, Srinivasalu S, Muthuraj S, Ram-Mohan V, Rajeshwara-Rao N (2008) Acid-leachable trace metals in sediments from an industrialized region (Ennore Creek) of Chennai City, SE coast of India: An approach towards regular monitoring. Estu. Coast. Shelf Sci. 692-703. https://doi.org/10.1016/j.ecss.2007.07.035

Khan R, Islam HMT, Islam ARMT (2021) Mechanism of elevated radioactivity in Teesta river basin from Bangladesh: Radiochemical characterization, provenance and associated hazards. Chemosphere. 264 (1):128459. doi: 10.1016/j.chemosphere.2020.128459.

Koide M, Brulan KW, Goldberg ED (1973) Th-228/Th-232 and Pb-210 geochronologies in marine and lake sediment. Geochim Cosmochim Acta 37 (5):1171–1187. DOI: 10.1016/0016-7037(73)90054-9

Li F, Mao L, Jia Y, Gu Z, Shi W, Chen L, Ye H (2018) Distribution and risk assessment of trace metals in sediments from Yangtze River estuary and Hangzhou Bay, China. Environ. Sci. Pollut. Res. 25(1), 855-866.

Loring DH, Rantala RTT (1992) Manual for the geochemical analyses of marine sediments and suspended particulate matter. Earth. Sci. Rev. 32, 235-316. http://dx.doi.org/10.1016/0012-8252(92)90001-A

Maanan M, Zourarah B, Sahabi M, Maanan M, Le Roy P, Mehdi K, Salhi F (2015) Environmental risk assessment of the Moroccan Atlantic continental shelf: the role of the industrial and urban area. Sci Total Environ. 511:407-15. doi: 10.1016/j.scitotenv.2014.12.098.

Magesh NS, Chandrasekar N, Vetha Roy D (2011) Spatial analysis of trace element contamination in sediments of Tamiraparani estuary, southeast coast of India. Estuar Coast Shelf Sci 92. 618-628 doi:10.1016/j.ecss.2011.03.001

Muller PJ, Suess E (1979) Productivity, sedimentation rate, and sedimentary organic matter in oceans- I organic carbon preservation. Deep-Sea Res. 26(12), pp.1347-1362

Pejman A, Bidhendi GN, Ardestani M, Saeedi M, Baghvand A (2015) A new index for assessing heavy metals contamination in sediments: A case study. Ecol. Indic.58, pp.365-373.

Ramasamy V, Senthil S, Meenakshisundaram V, Gajendran V (2009) “Measurement of natural radioactivity in beach sediments from the northeast coast of Tamil Nadu, India”. Res. J. Appl. Sci. Eng. Tech. 1(2), pp.54-58.

Ravisankar R, Vanasundari K, Suganya M, Raghu Y, Rajalakshmi A, Chandrasekaran A, Sivakumar S, Chandramohan J, Vijayagopal P, Venkatraman B (2014) Multivariate statistical analysis of radiological data of building materials used in Tiruvannamalai, Tamilnadu, India. Appl. Radiat. Isot. 85, pp.114-127.

Senthilkumar B, Dhavamani V, Ramkumar S, Philominathan P (2010) Measurement of gamma radiation levels in soil samples from Thanjavur using gamma-ray spectrometry and estimation of population exposure. J. Med. Phys. 35(1), 48–53. https://doi.org/10.4103/0971-6203.55966

Sérgio LR Sêco, Alcides JSC Pereira, Luís V Duarte, Filipa P Domingos (2021) Sources of uncertainty in field gamma-ray spectrometry: Implications for exploration in the Lower-Middle Jurassic sedimentary succession of the Lusitanian Basin (Portugal), J. Geochem. Explor. 227, 106799, https://doi.org/10.1016/j.gexplo.2021.106799.

Stamatis N, Kamidis N, Pigada P, Sylaios G, Koutrakis E (2019) Quality Indicators and Possible Ecological Risks of Heavy Metals in the Sediments of three Semi-closed East Mediterranean Gulfs. Toxics. 7(2):30. doi: 10.3390/toxics7020030.

Sylaios G, Kamidis N, Stamatis N (2012) Assessment of Trace Metals Contamination in the Suspended Matter and Sediments of a Semi-enclosed Mediterranean Gulf, Soil Sediment Contam.21:6, 673-700, DOI: 10.1080/15320383.2012.691128

Taieb Errahmani D, Noureddine A, Abril-Hernández JM, Boulahdid M (2020) Environmental radioactivity in a sediment core from Algiers Bay: Radioecological assessment, radiometric dating and pollution records. Quat Geochronol. 56, 101049. https://doi.org/10.1016/j.quageo.2019.101049.

Taylor SR, Mclennan SM (1995) The geochemical evolution of the continental crust. Rev Geophys. 33(2), pp.241-265.

Thangam V, Rajalakshmi A, Chandrasekaran A, Jananee B (2020) Radiometric analysis of some building materials using gamma ray spectrometry. J. Radioanal. Nucl. Chem. 324:1059–1067. https://doi.org/10.1007/s10967-020-07175-9.

Thangam V, Rajalakshmi A, Chandrasekaran A, Jananee B (2020) Measurement of natural radioactivity in river sediments of Thamirabarani, Tamilnadu, India using the gamma-ray spectroscopic technique. Int. J. Environ. An. Ch. DOI: 10.1080/03067319.2020.1722815.

589 Tholkappian M, Chandrasekaran A, Harikrishnan N, Ganesh D, Elango G, Ravisankar R
590 (2017) Measurement of natural radioactivity in and around Chennai Coast, East Coast of Tamil
591 Nadu, India, using gamma ray spectrometry. Radiat. Prot. Environ. 40(1), p.9.

592 Tholkappian M, Ganesh D, Devanesan E, Harikrishnan N, Jebakumar JPP, Ravisankar R
593 (2018) Data on natural radioactivity and associated radiation hazards in coastal sediment of
594 Chennai Coast, Tamilnadu, India using gamma ray spectrometry. Data Br. 17, pp.551-558.

595 Tian K, Huang B, Xing Z, Hu W (2017) Geochemical baseline establishment and ecological
596 risk evaluation of heavy metals in greenhouse soils from Dongtai, China. Ecol. Indic. 72,
597 pp.510-520.

598 Tomlinson DL, Wilson JG, Harris CR, Jeffrey DW (1980) Problems in the assessment of
599 heavy-metal levels in estuaries and the formation of a pollution index. Helgoland Mar. Res.
600 33(1-4), pp.566-575.

601 UNSCEAR (2000) United Nations Scientific Committee on the Effects of Atomic Radiation
602 (UNSCEAR), New York. Sources and effects of ionizing radiation UNSCEAR 2000 report to
603 the General Assembly, with scientific annexes Volume I: Sources. United Nations (UN): UN.
604 657 p; UN; New York, NY (United States); ISBN 92-1-142238-8.

605 Wang X, Liu B, Zhang W (2020) Distribution and risk analysis of heavy metals in sediments
606 from the Yangtze River Estuary, China. Environ Sci Pollut Res Int. 27(10):10802-10810. doi:
607 10.1007/s11356-019-07581-x.

608 Wang Y, Yang Z, Shen Z, Tang Z, Niu J, Gao F (2011) Assessment of heavy metals in
609 sediments from a typical catchment of the Yangtze River, China Environ. Monit. Assess.
610 172(1), pp.407-417.

611 Yii MW, Zaharudin A, Abdul-Kadir I (2009) Distribution of naturally occurring radionuclides
612 activity concentration in East Malaysian marine sediment. Appl Radiat Isot. 67(4):630-5. doi:
613 10.1016/j.apradiso.2008.11.019.

614 Zhang L, Li X, Wang M, He Y, Chai L, Huang J, Wang H, Wu X, Lai Y (2016) Highly Flexible
615 and Porous Nanoparticle-Loaded Films for Dye Removal by Graphene Oxide-Fungus
616 Interaction. ACS. Appl. Mater. Interfaces. 8(50):34638-34647. doi: 10.1021/acsami.6b10920.

617 Zhou Z, Yang Z, Sun Z, Liao Q, Guo Y, Chen, J (2020) Multidimensional pollution and
618 potential ecological and health risk assessments of radionuclides and metals in the surface soils

of a uranium mine in East China. J. Soils Sediments. 20(2), pp.775-791. https://doi.org/10.1007/s11368-019-02428-x

Credit authorship contribution statement:

Manikanda Bharath Karuppasamy: Conceptualization, Formal analysis, Methodology, Software, Investigation, Writing - original draft, Writing - review & editing. **Usha Natesan:** Writing - review & editing. **Chandrasekaran Seethapathy:** Resources, Project administration, Investigation and Writing - review & editing. **Srinivasalu Seshachalam:** Supervision, Project administration and Funding acquisition**.**

Declaration of interests

☒ The authors declare that they have no known competing financial interests or personal relationships that could have appeared to influence the work reported in this paper.

Figure captions

Fig. 1 The study area and sediment distribution with bathymetry details of sampling sites.
Fig. 2 Spatial distributions of primordial radionuclides and depositional environments of study area showing continental to marine zone.
Fig. 3 Spatial variation of radiological hazard effects (Gamma Dose Rate, Radium equivalent activity, Annual Effective Dose Equivalent, Activity Utilization Index, External hazard index, and Internal hazard index) in the study area.
Fig. 4 Spatial distribution of sediment characteristics of study area.
Fig. 5 Spatial distribution of evaluating the contamination status (Contamination Factor (CF), Contamination Degree (CD), Pollution Load Index (PLI)) and Box whisker Plot of heavy metals concentrations in the study area.
Fig. 6 Spatial variation of Potential ecological risk index in the study area.

649 **Table 1. Geo-accumulation Index (Igeo) of the elements of marine sediments off Coromandel**

650 **Coast in India**

Elements/location	Mn	Cr	Cu	Pb	Zn	Ni	Co	Fe
S1	-3.75	-0.55	0.88	-0.31	0.14	-1.91	2.43	-2.50
S2	-1.92	-0.56	1.85	-1.23	-0.23	-0.02	1.15	0.50
S3	-3.98	-0.95	0.82	0.41	-4.80	-1.47	2.27	1.01
S4	-2.60	-2.15	2.49	-3.29	-1.22	-5.32	2.71	-0.72
S5	-2.46	-2.57	2.58	-2.87	-0.92	-4.54	2.82	-0.42
S6	-2.82	1.27	0.55	-3.75	-0.28	-0.92	4.76	-0.07
S7	-2.59	0.78	1.51	-0.52	-0.21	0.06	-0.45	-5.05
S8	-4.40	-3.31	-0.07	-0.54	-0.76	-0.45	2.78	0.45
S9	-5.63	0.61	2.60	-3.47	-1.36	-0.83	1.18	-0.20
S10	-7.14	-1.25	1.66	-0.16	0.56	-3.12	3.60	0.08
S11	-4.11	1.77	1.62	0.03	-0.50	0.99	4.53	0.18
S12	-4.28	0.44	2.05	0.54	-0.16	1.01	3.33	-2.58
S13	-4.01	0.63	2.11	0.13	-0.12	1.16	3.39	0.76
S14	-3.21	1.30	1.40	-0.14	-2.03	-0.25	-0.64	0.92
S15	-3.25	0.31	2.55	-0.43	-1.14	0.72	3.73	-1.66
S16	-5.36	0.87	1.55	-0.31	-2.53	0.58	2.99	-1.87
S17	-5.98	0.82	-1.07	-4.53	-0.25	0.22	2.77	-1.31
S18	-3.73	-1.12	3.19	1.06	0.06	1.03	2.96	-0.80
S19	-3.66	-0.62	3.14	0.13	0.23	1.19	2.99	-0.34
S20	-2.37	-1.95	-1.94	0.46	-2.58	0.63	0.26	0.41
S21	-3.02	1.11	1.59	0.39	-0.20	-2.12	3.29	-0.79
S22	-3.07	-4.42	1.53	-1.62	0.01	-1.71	2.67	-1.47
S23	-2.91	1.09	1.51	0.17	-0.08	0.62	4.44	-0.76
S24	-4.56	0.41	1.62	-0.58	0.58	0.27	3.27	0.28
S25	-4.19	0.47	1.80	-0.21	-0.47	0.60	3.33	-0.13
S26	-3.09	-2.53	3.33	0.49	-2.60	-0.24	4.15	0.01

Value	Contamination level
Igeo< 0	Uncontaminated
0 - 1	Uncontaminated to moderately contaminated
1 - 2	Moderately contaminated

2 - 3	Moderately to heavily contaminated
3 - 4	Heavily contaminated
– 5 and >5	Heavily to extremely contaminated

651

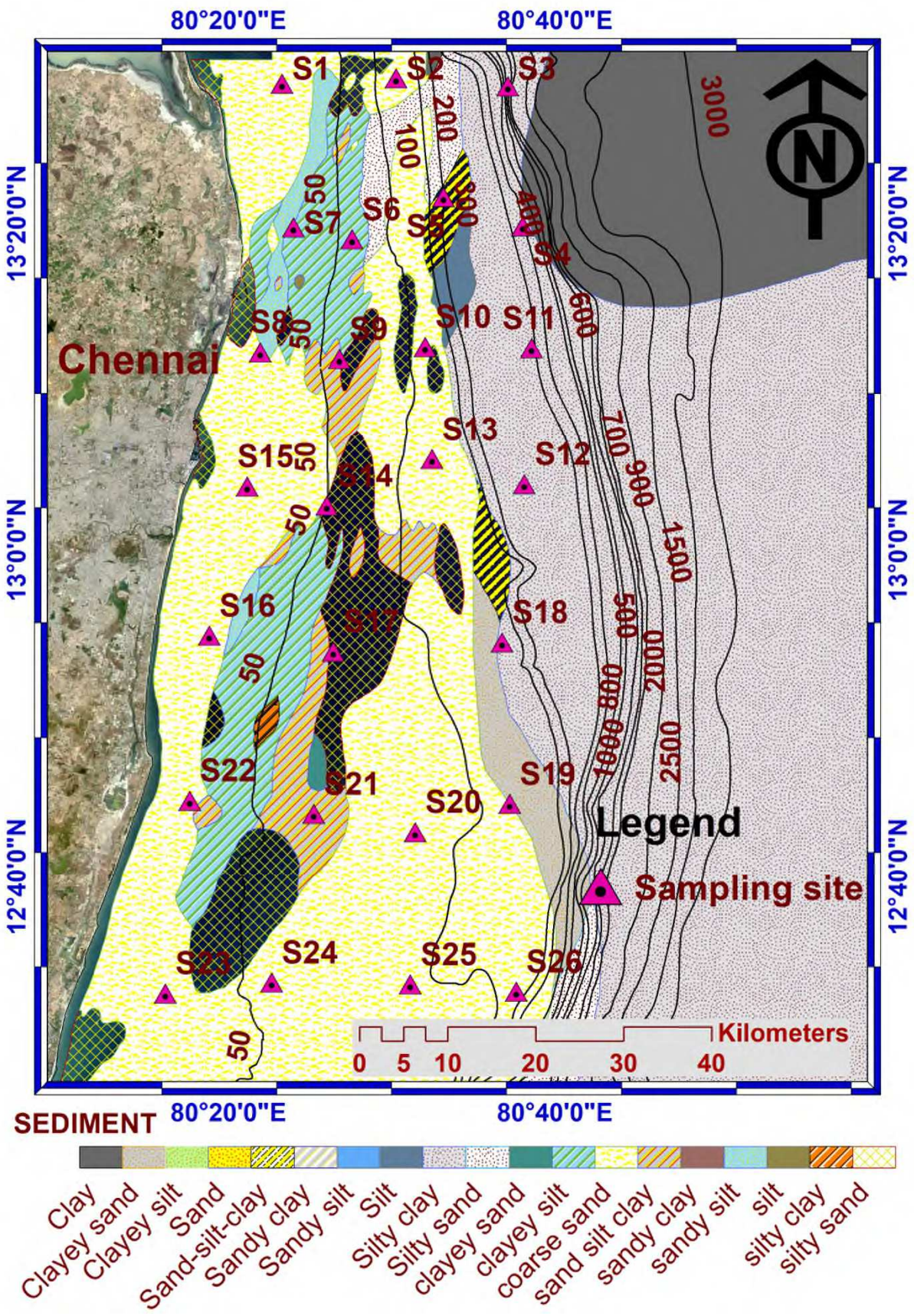

Fig. 1 The study area and sediment distribution with bathymetry details of sampling sites.

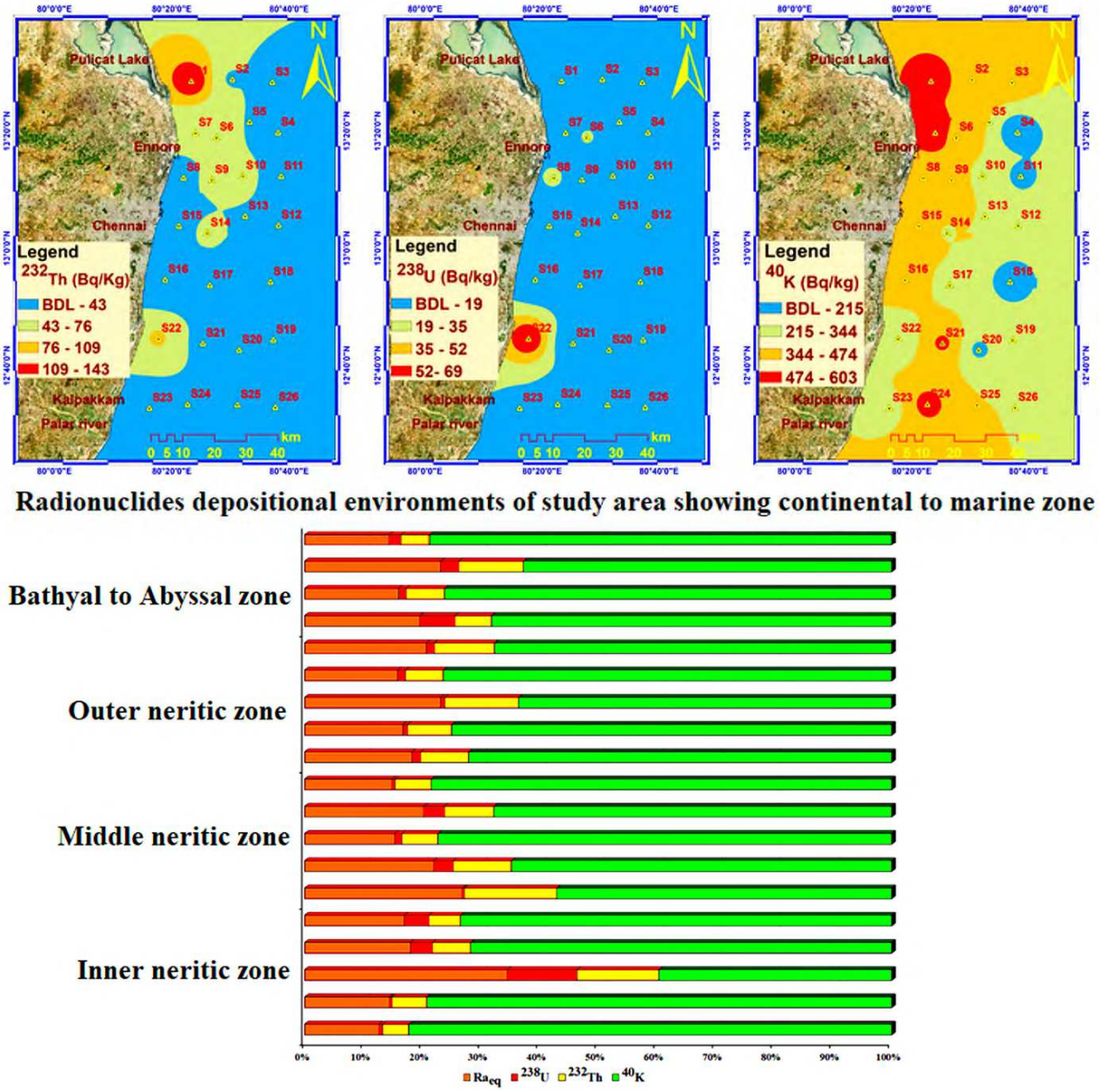

Fig. 2 Spatial distributions of primordial radionuclides and depositional environments of study area showing continental to marine zone.

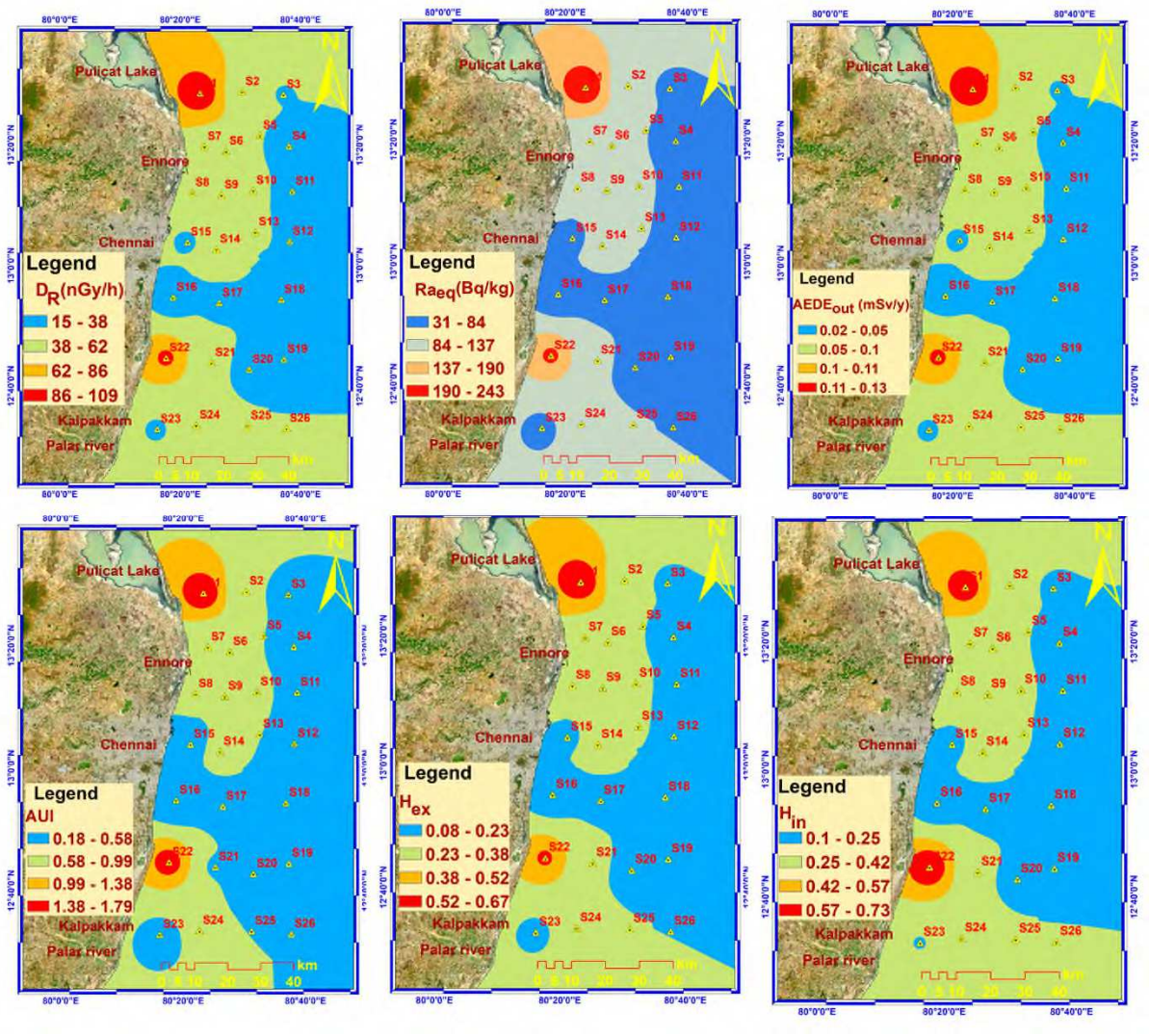

Fig. 3 Spatial variation of radiological hazard effects (Gamma Dose Rate, Radium equivalent activity, Annual Effective Dose Equivalent, Activity Utilization Index, External hazard index, and Internal hazard index) in the study area.

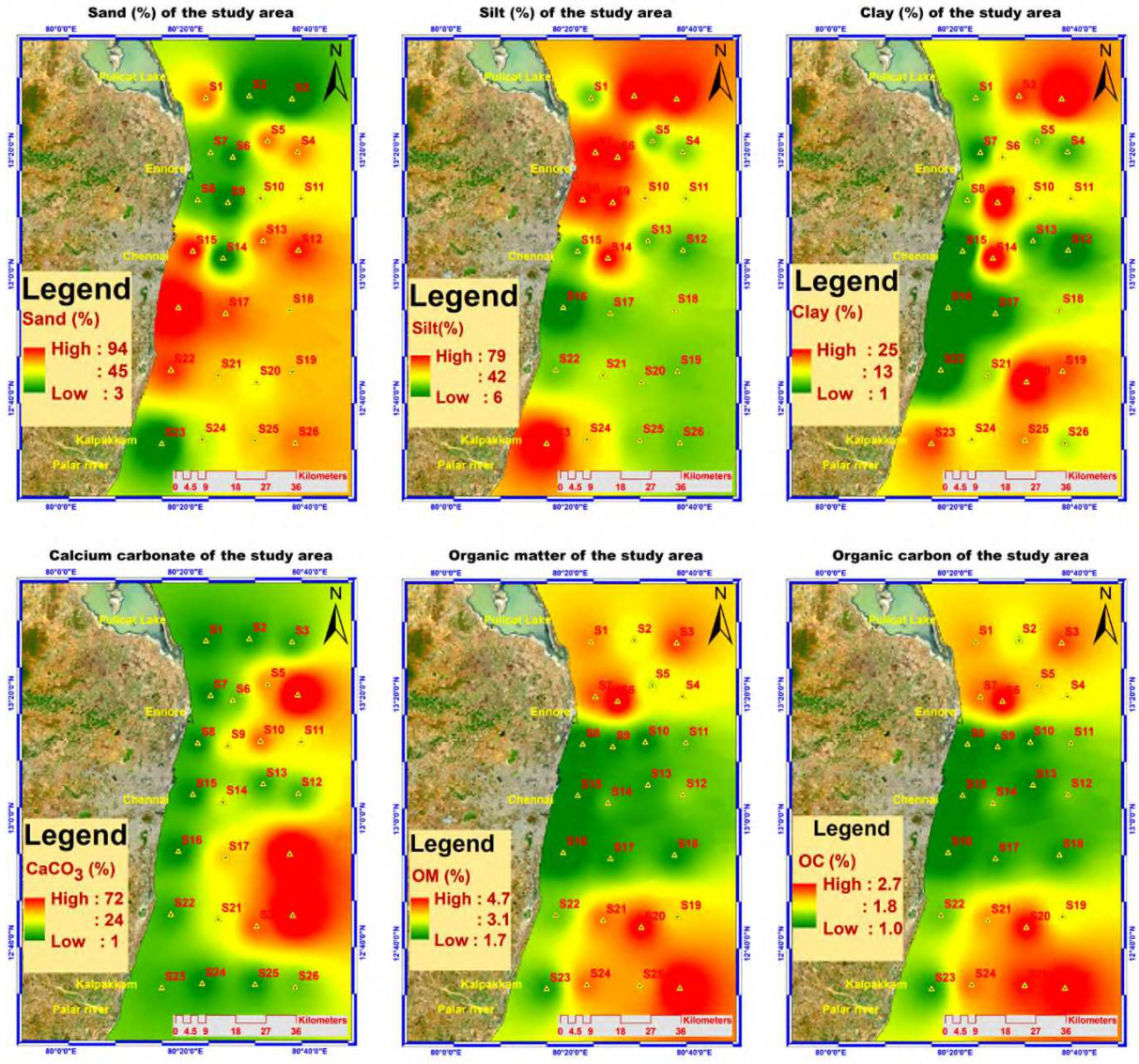

Fig. 4 Spatial distribution of sediment characteristics of study area.

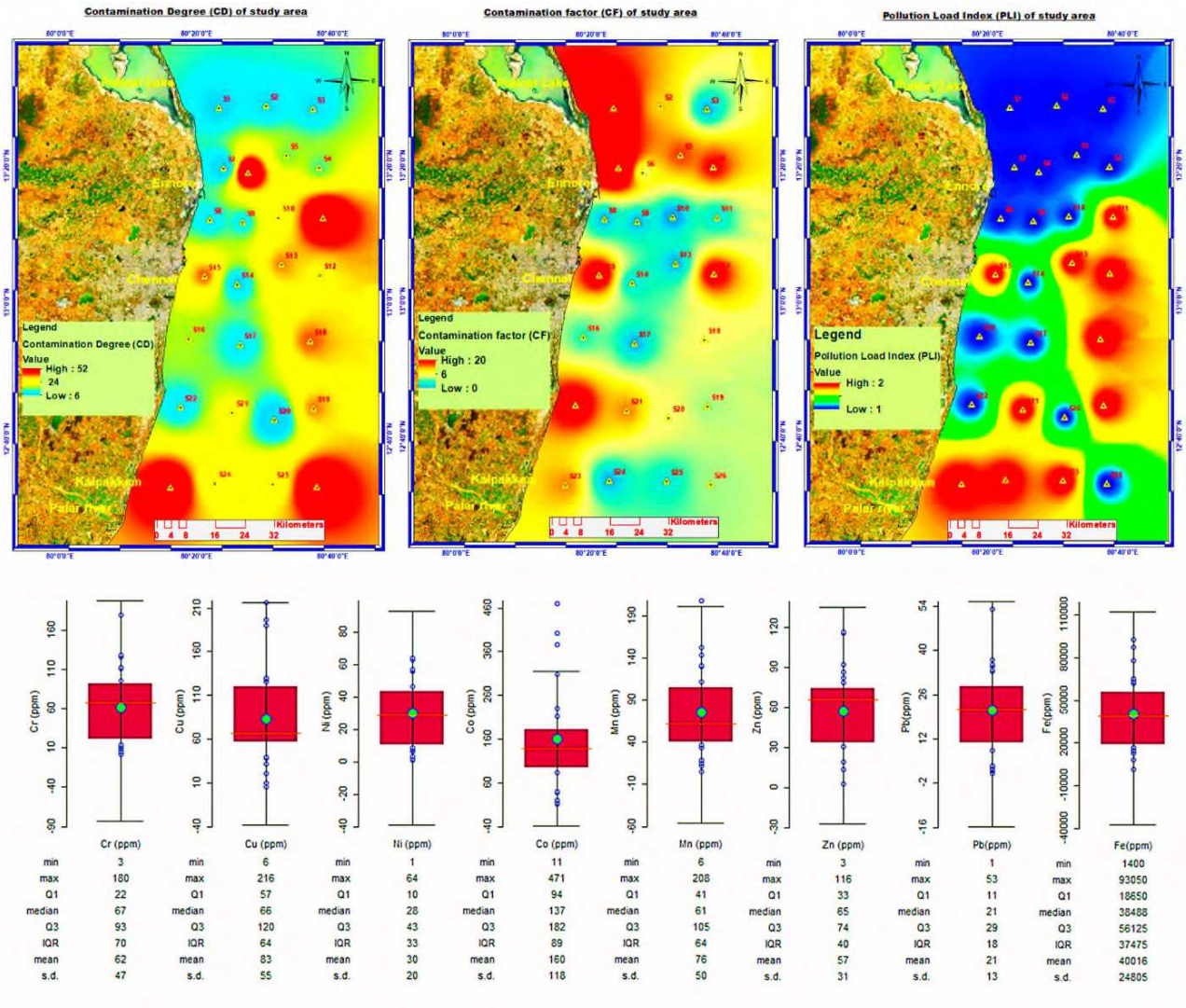

	Cr (ppm)	Cu (ppm)	Ni (ppm)	Co (ppm)	Mn (ppm)	Zn (ppm)	Pb(ppm)	Fe(ppm)
min	3	6	1	11	6	3	1	1400
max	180	216	64	471	208	116	53	93050
Q1	22	57	10	94	41	33	11	18650
median	67	66	28	137	61	65	21	38488
Q3	93	120	43	182	105	74	29	56125
IQR	70	64	33	89	64	40	18	37475
mean	62	83	30	160	76	57	21	40016
s.d.	47	55	20	118	50	31	13	24805

Fig. 5 Spatial distribution of evaluating the contamination status (Contamination Factor (CF), Contamination Degree (CD), Pollution Load Index (PLI)) and Box whisker Plot of heavy metals concentrations in the study area.

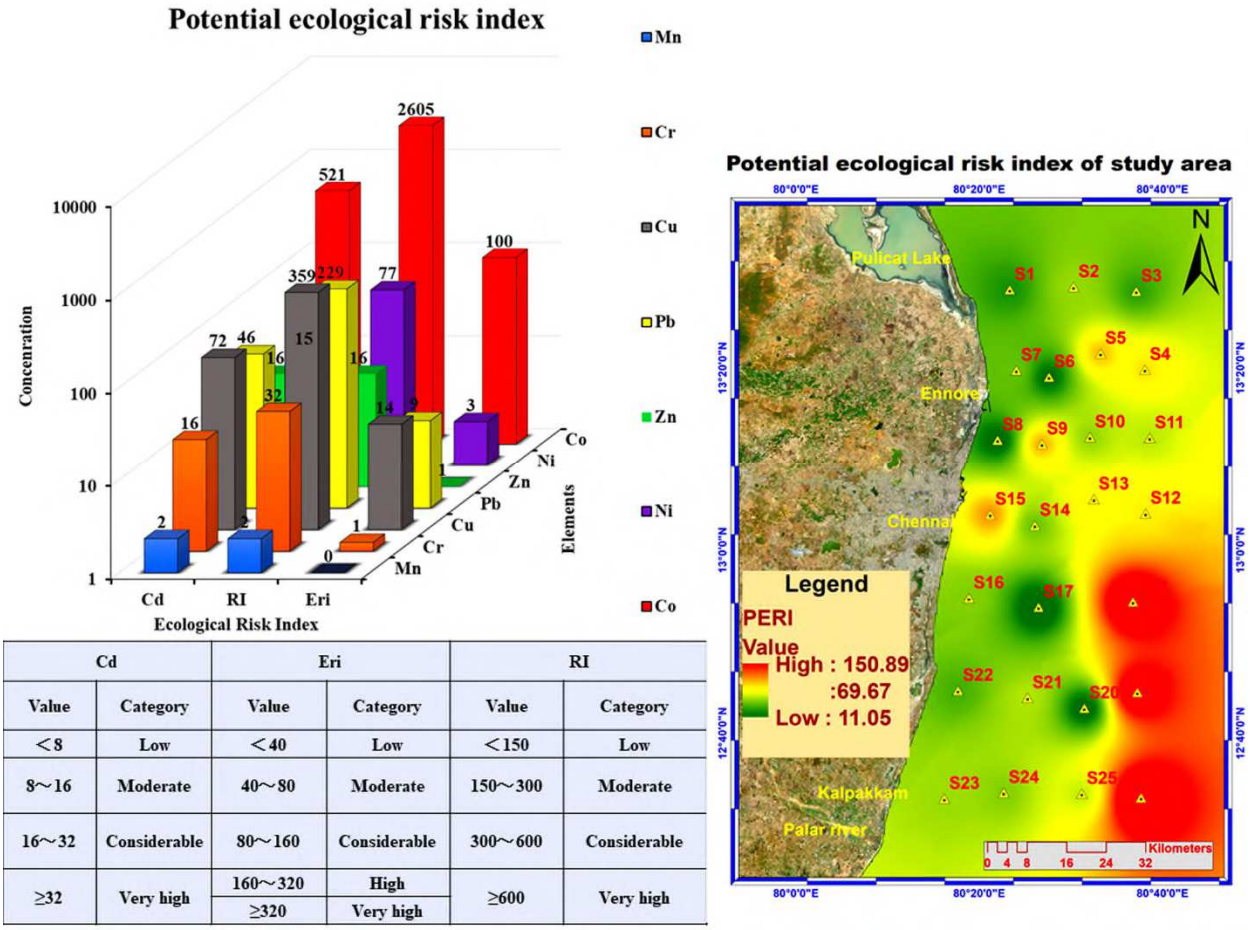

Cd		Eri		RI	
Value	Category	Value	Category	Value	Category
<8	Low	<40	Low	<150	Low
8~16	Moderate	40~80	Moderate	150~300	Moderate
16~32	Considerable	80~160	Considerable	300~600	Considerable
≥32	Very high	160~320	High	≥600	Very high
		≥320	Very high		

Fig. 6 Spatial variation of Potential ecological risk index in the study area.

Supplementary Files

This is a list of supplementary files associated with this preprint. Click to download.

- Supplements.docx